Cell Reports, Volume *37*

Supplemental information

NuMorph: Tools for cortical cellular phenotyping in tissue-cleared whole-brain images

Oleh Krupa, Giulia Fragola, Ellie Hadden-Ford, Jessica T. Mory, Tianyi Liu, Zachary Humphrey, Benjamin W. Rees, Ashok Krishnamurthy, William D. Snider, Mark J. Zylka, Guorong Wu, Lei Xing, and Jason L. Stein

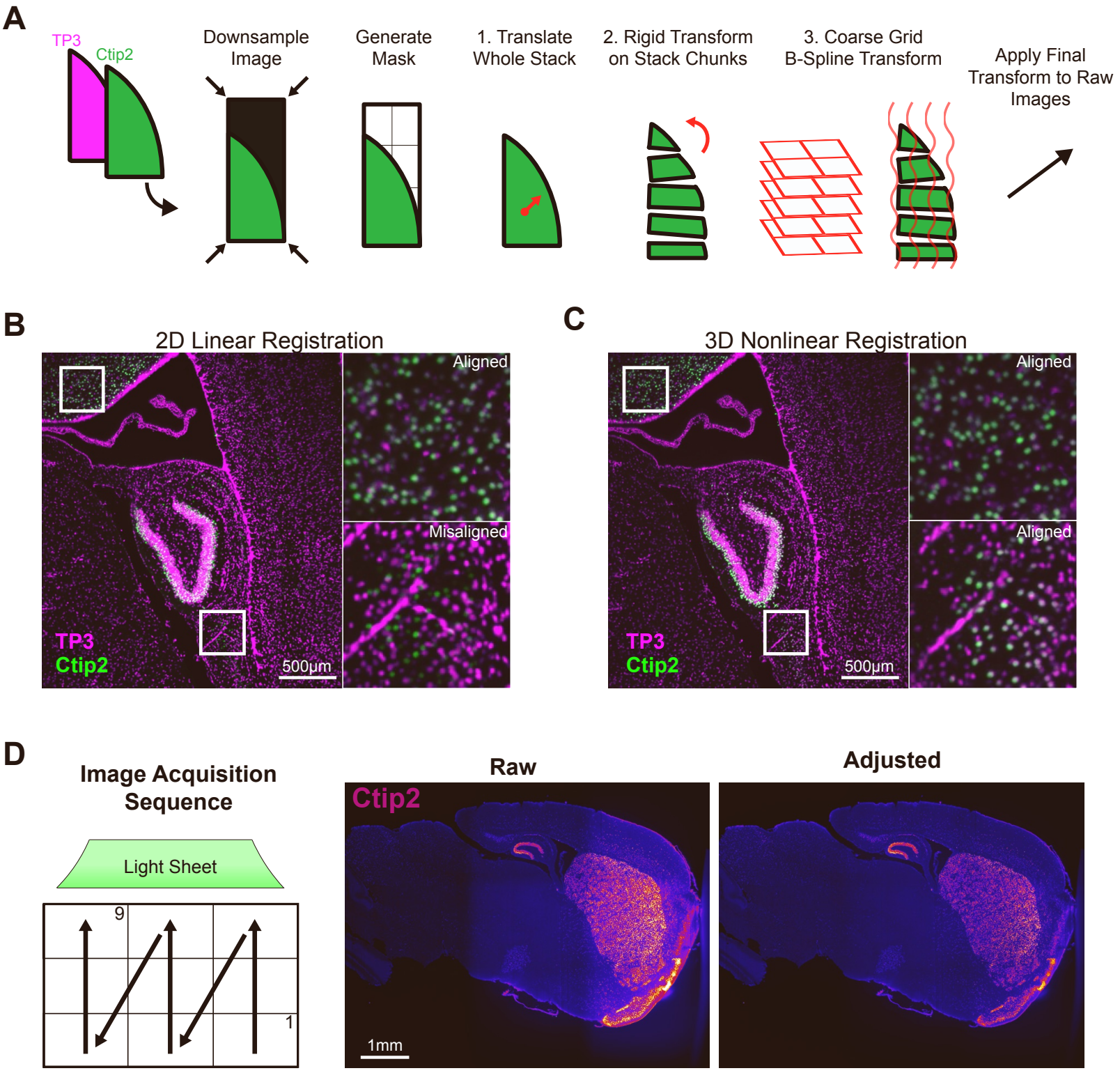

Figure S1. Nonlinear Alignment and Intensity Adjustment of 3D Multichannel Images, Related to Figure 1.

A. Overview of alignment procedures.

B. Example of channel misalignment after 2D registration by translation showing only part of the image aligning correctly. Scale bars = 500μm.

C. Same section as in B after the nonlinear alignment procedure.

D. *Top1* cKO sample images of Ctip2 labeling with (right) or without (left) adjusting intensities for tile positions and light-sheet width. Scale bar = 1mm.

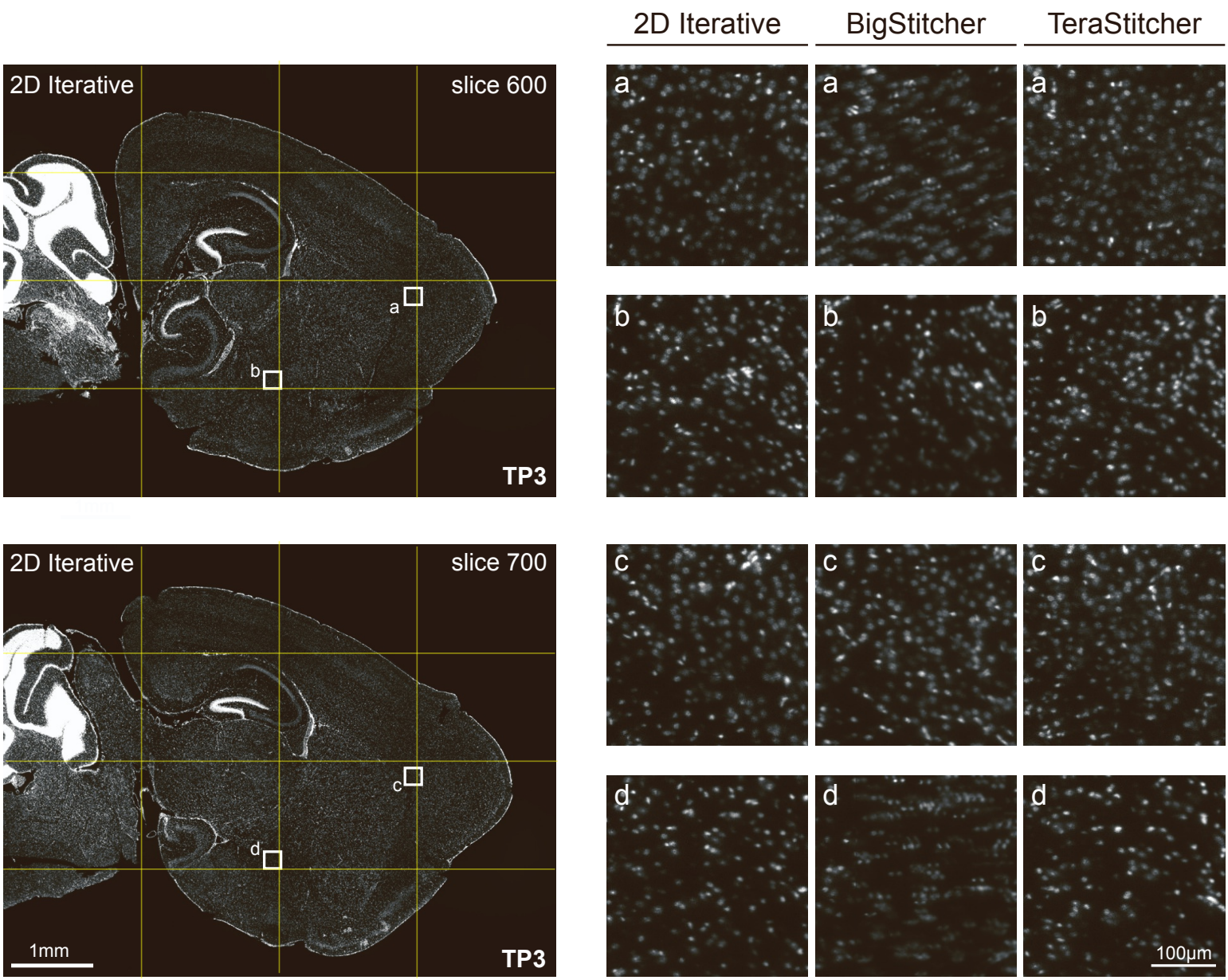

Figure S2. Iterative 2D Stitching of Multi-Tile Light Sheet Images, Related to Figure 1.
Sample results from 2D iterative stitching of WT mouse hemisphere compared with other dedicated 3D stitching software. Yellow lines indicate approximate stitching seams. Scale bar = 1mm; inserts = 100µm.

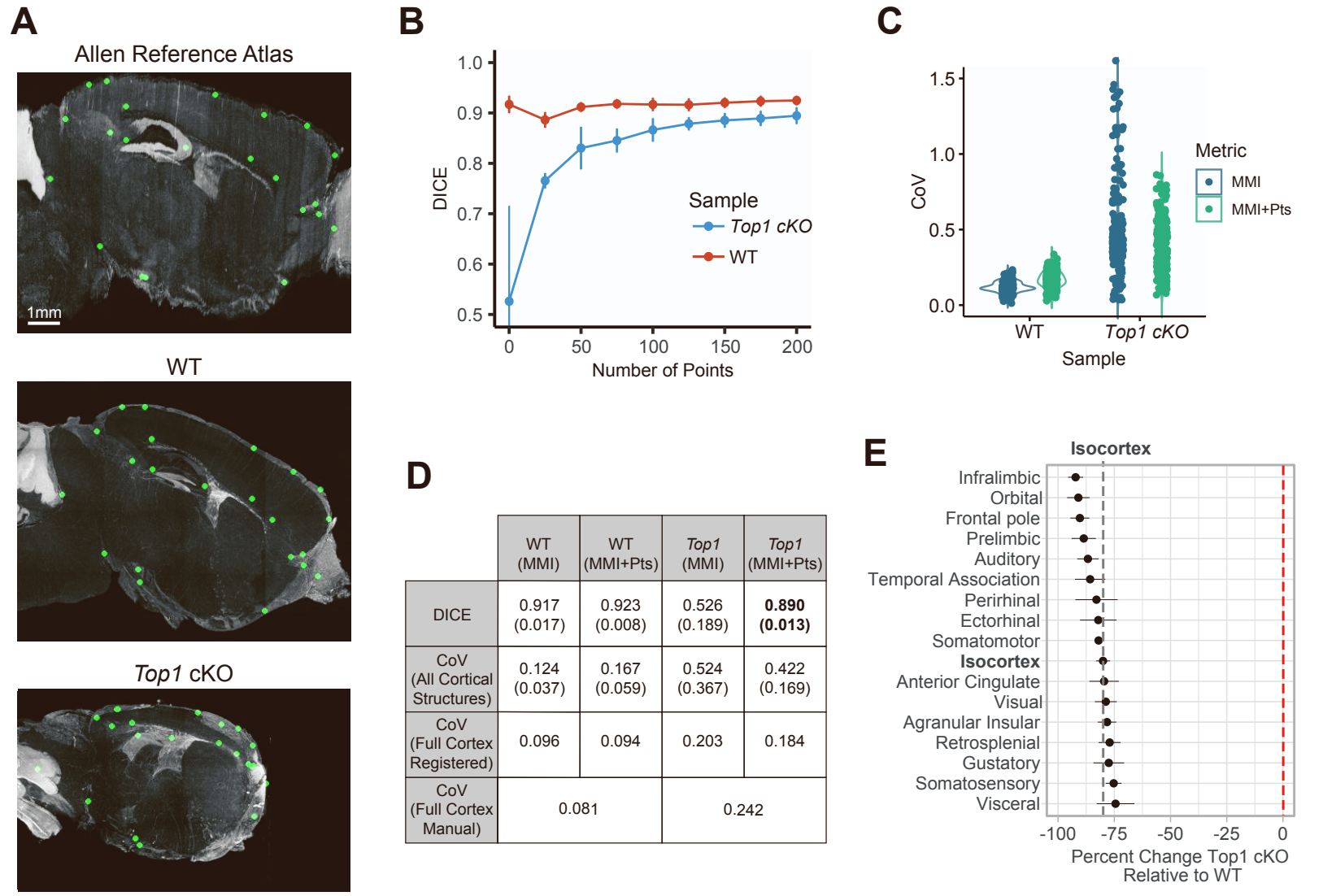

D

	WT (MMI)	WT (MMI+Pts)	*Top1* (MMI)	*Top1* (MMI+Pts)
DICE	0.917 (0.017)	0.923 (0.008)	0.526 (0.189)	**0.890 (0.013)**
CoV (All Cortical Structures)	0.124 (0.037)	0.167 (0.059)	0.524 (0.367)	0.422 (0.169)
CoV (Full Cortex Registered)	0.096	0.094	0.203	0.184
CoV (Full Cortex Manual)	0.081		0.242	

Figure S3. Image Landmark Selection for Points-Guided Image Registration, Related to Figure 2.
A. 1 mm thick sagittal maximum intensity projection displaying corresponding points positions in ARA, WT, and *Top1* cKO brain hemispheres. Scale bar = 1mm.
B. DICE scores measuring cortical registration accuracy in WT and *Top1* cKO samples based on the number of points used to guide registration. Measurements with no corresponding points were made using affine + b-spline registration without a points distance metric. Data represented as mean ± standard deviation.
C. Coefficients of variation (CoV) of structure volumes for all cortical annotations in the ARA after registration with or without corresponding points.
D. DICE scores and CoV metrics for indicated registration procedures. Data represented as mean (± standard deviation). CoV was calculated for individual ARA annotations (242 structures plotted in B) or the full isocortex after registration. These are compared with the CoV for the full cortex based on manual annotation. Bold value: *Top1* MMI/Top1 MMI+ Pts, $p < 0.001$.
E. Percent change in cortical region volumes in *Top1* cKO samples compared to WT. Dashed line indicates average change across the entire cortex. Data represented as mean ± SEM.

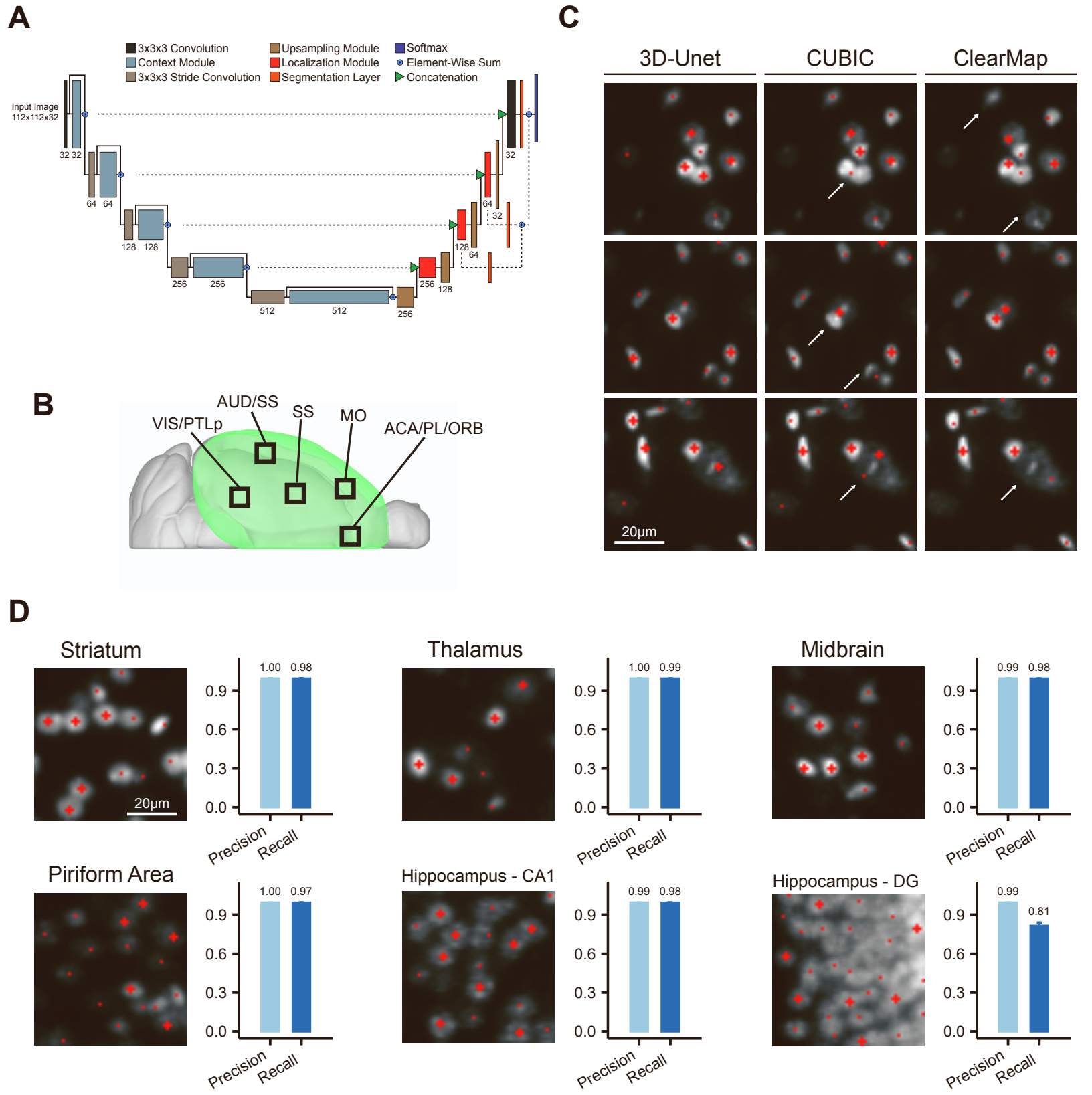

Figure S4. 3D-Unet Training and Evaluation, Related to Figure 2.

A. 3D-Unet architecture adapted from (36).

B. Approximate patch locations used for training the 3D-Unet nuclei detection model

C. Example images of nuclei detection results. Cross symbols indicate centroids in the displayed z slice whereas points indicate centroids in slices directly above or below. Arrows indicate detection errors in the full 3D volume. Scale bar = 20μm.

D. Precision and recall of nuclei detection in non-cortical brain regions. Results plotted are as mean ± standard deviation of 3 samples in 242x242x200 μm patches. (DG: dentate gyrus). Scale bar = 20μm.

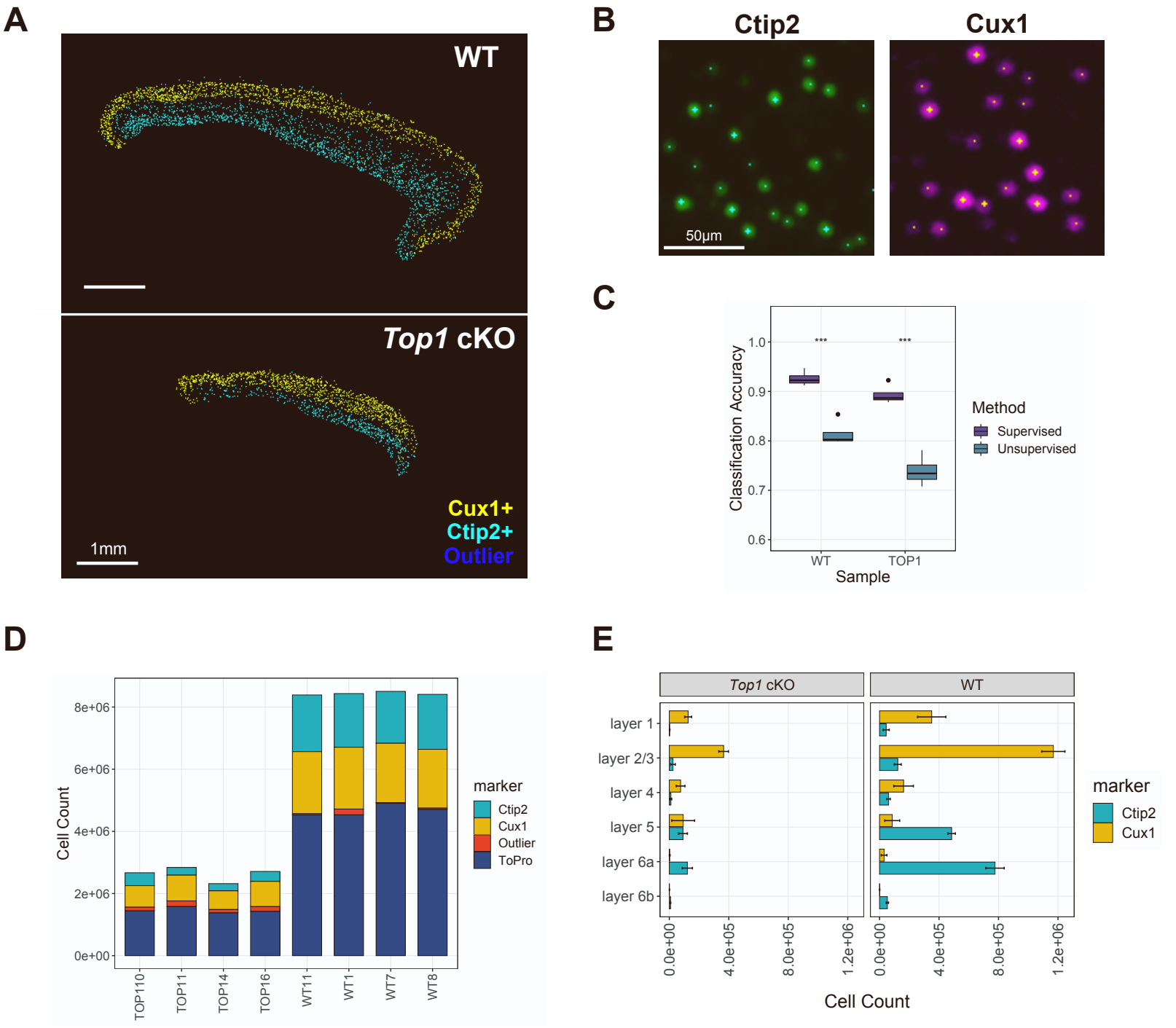

Figure S5. Cell-type Classification using Supervised SVM Classifier, Related to Figure 3.

A. Cell-type positions for upper and lower layer cortical neurons in a sagittal section for WT and *Top1* cKO after SVM classifications. Scale bar = 1mm.

B. Representative images of Ctip2+ and Cux1+ cell-type classification using SVM. Cross symbols indicate centroids in the displayed z slice whereas points indicate centroids in slices directly above or below. Scale bar = 50μm.

C. Classification accuracies using a trained SVM (supervised) classifier or by Gaussian Mixture Modeling (unsupervised). Accuracy is measured as the fraction of 1,000 cells in each sample with the correct classification based on manual identification. SVM accuracies determined based on 5-fold cross-validation. (***p < 0.001; McNemar test).

D. Total counts for each cell-type classification in WT and *Top1* cKO samples.

E. Distributions of Ctip2+ and Cux1+ cells across cortical layers (mean ± standard deviation).

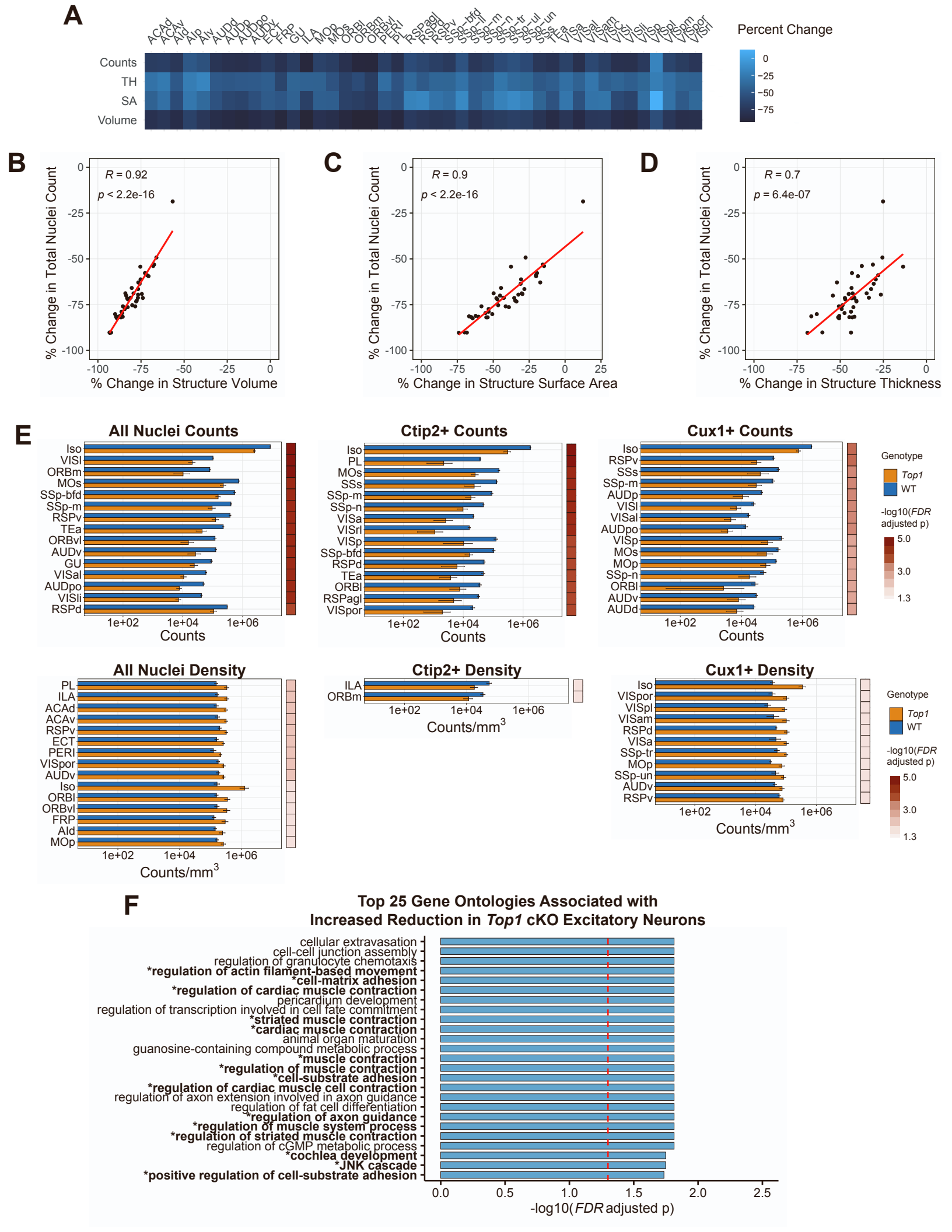
A
ACAd ACAv AId AIp AIv AUDd AUDp AUDpo AUDv ECT FRP GU ILA MOp MOs ORBl ORBm ORBvl PERI PL RSPagl RSPd RSPv SSp-bfd SSp-ll SSp-m SSp-n SSp-tr SSp-ul SSp-un SSs TEa VISa VISal VISam VISC VISli VISp VISpl VISpm VISpor VISrl
Counts
TH
SA
Volume
Percent Change
0
−25
−50
−75
B
R = 0.92
p < 2.2e-16
% Change in Total Nuclei Count
% Change in Structure Volume
C
R = 0.9
p < 2.2e-16
% Change in Total Nuclei Count
% Change in Structure Surface Area
D
R = 0.7
p = 6.4e-07
% Change in Total Nuclei Count
% Change in Structure Thickness
E
All Nuclei Counts
Iso VISl ORBm MOs SSp-bfd SSp-m RSPv TEa ORBvl AUDv GU VISal AUDpo VISli RSPd
1e+02 1e+04 1e+06
Counts
Ctip2+ Counts
Iso PL MOs SSs SSp-m SSp-n VISa VISrl VISp SSp-bfd RSPd TEa ORBl RSPagl VISpor
1e+02 1e+04 1e+06
Counts
Cux1+ Counts
Iso RSPv SSs SSp-m AUDp VISl VISal AUDpo VISp MOs MOp SSp-n ORBl AUDv AUDd
1e+02 1e+04 1e+06
Counts
Genotype
Top1
WT
-log10(FDR adjusted p)
5.0
3.0
1.3
All Nuclei Density
PL ILA ACAd ACAv RSPv ECT PERI VISpor AUDv Iso ORBl ORBvl FRP AId MOp
1e+02 1e+04 1e+06
Counts/mm3
Ctip2+ Density
ILA ORBm
1e+02 1e+04 1e+06
Counts/mm3
Cux1+ Density
Iso VISpor VISpl VISam RSPd VISa SSp-tr MOp SSp-un AUDv RSPv
1e+02 1e+04 1e+06
Counts/mm3
Genotype
Top1
WT
-log10(FDR adjusted p)
5.0
3.0
1.3
F
Top 25 Gene Ontologies Associated with Increased Reduction in Top1 cKO Excitatory Neurons
cellular extravasation
cell-cell junction assembly
regulation of granulocyte chemotaxis
*regulation of actin filament-based movement
*cell-matrix adhesion
*regulation of cardiac muscle contraction
pericardium development
regulation of transcription involved in cell fate commitment
*striated muscle contraction
*cardiac muscle contraction
animal organ maturation
guanosine-containing compound metabolic process
*muscle contraction
*regulation of muscle contraction
*cell-substrate adhesion
*regulation of cardiac muscle cell contraction
regulation of axon extension involved in axon guidance
regulation of fat cell differentiation
*regulation of axon guidance
*regulation of muscle system process
*regulation of striated muscle contraction
regulation of cGMP metabolic process
*cochlea development
*JNK cascade
*positive regulation of cell-substrate adhesion
0.0 0.5 1.0 1.5 2.0 2.5
-log10(FDR adjusted p)

Figure S6. Structural and Molecular Associations with Cell Loss in the *Top1* cKO Model, Related to Figures 3 and 4.

A. Heatmap displaying percent change in cortical cell count, volume, surface area, and thickness for each cortical region.

B-D. Correlation between total cell count difference and volume (B), surface area (C), and thickness (D) across cortical regions.

E. Comparison of cell-type counts or densities between WT and *Top1* cKO across cortical regions and the full isocortex. Displaying the top 15 structures (FDR < 0.05) binned by significance level and sorted by absolute difference in count or density within each bin. Data represented as mean ± standard deviation and plotted on log10 scale. Structure name abbreviations provided in Table S1.

F. Gene ontology showing the top 25 most significant categories correlated with neuron loss in *Top1* cKO. Bolded categories contain at least 1 gene differentially expressed in *Top1* cKO from scRNA-seq studies.

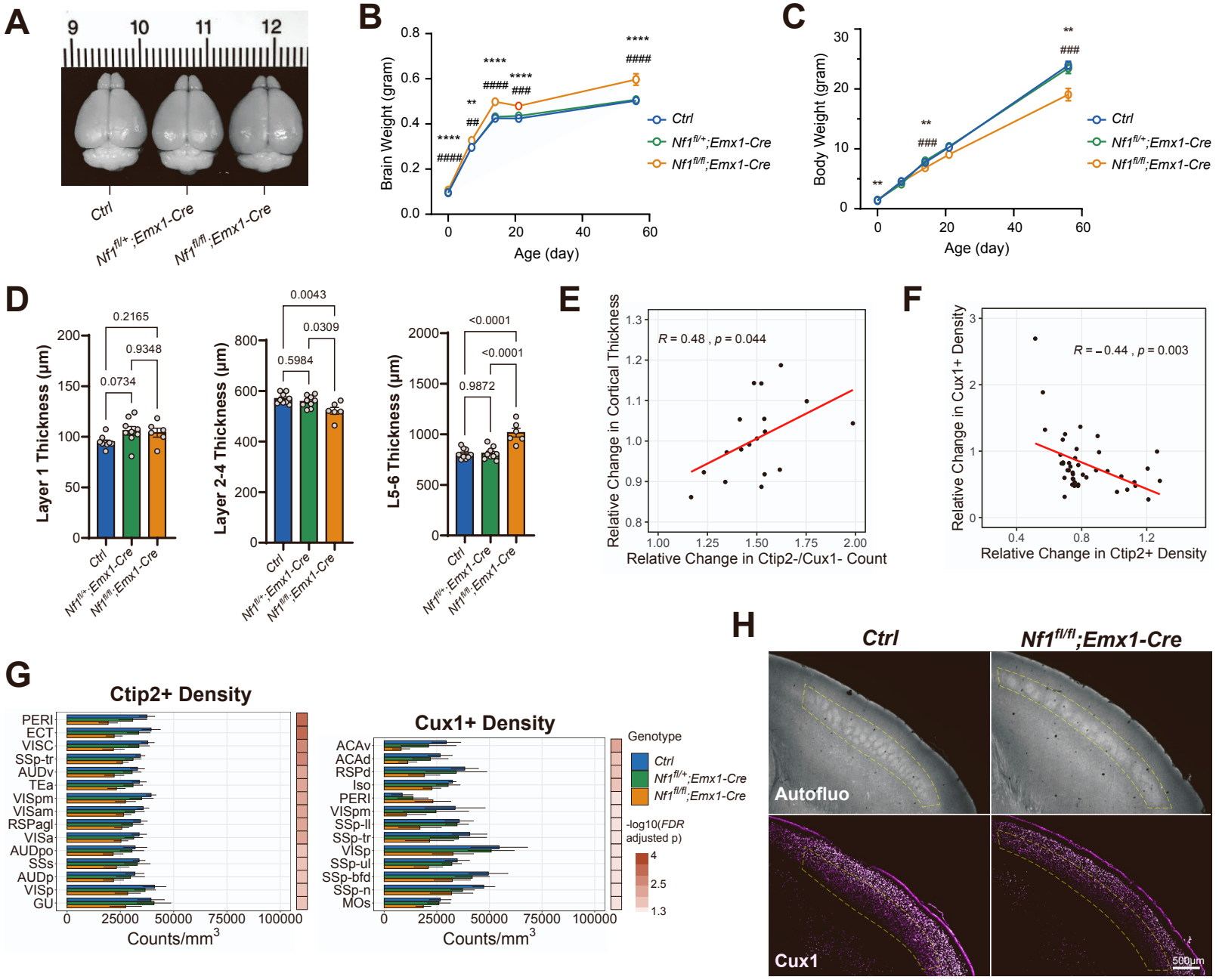

Figure S7. Characterization of *Nf1* cKO Models and Structural Associations with Cortical Cell-type Densities, Related to Figures 5-7.

A. Representative images of P14 brains from *Ctrl*, *Nf1$^{fl/+}$;Emx1-Cre*, and *Nf1$^{fl/fl}$;Emx1-Cre* mice. Scale = mm/cm.

B-C. Brain and body weight measurements for *Ctrl*, *Nf1$^{fl/+}$;Emx1-Cre*, and *Nf1$^{fl/fl}$;Emx1-Cre* mice at multiple developmental time points (mean ± SEM; *Nf1$^{fl/fl}$;Emx1-Cre* vs Ctrl: **, p<0.01, ***, p<0.001, ****, p<0.0001; *Nf1$^{fl/fl}$;Emx1-Cre* vs *Nf1$^{fl/+}$;Emx1-Cre*: ##, p<0.01, ###, p<0.001, ####, p<0.0001).

D. Quantification of cortical layer thickness in *Nf1* models from 2D sections of somatosensory cortex (mean ± SEM).

E. Association between cortical thickness and relative change in Ctip2-/Cux1- cell counts in the *Nf1$^{fl/fl}$;Emx1-Cre* model. (R: Pearson's correlation coefficient).

F. Association between relative change in Cux1+ and Ctip2+ cell densities in the *Nf1$^{fl/fl}$;Emx1-Cre* model. (R: Pearson's correlation coefficient).

G. Differences in cell densities of Ctip2+ and Cux1+ cells across 43 cortical regions and the full isocortex after *Nf1* deletion. The top 15 structures sorted by binned p-value and fold change are shown (*Nf1$^{fl/fl}$;Emx1-Cre* vs. Ctrl, mean ± standard deviation, FDR<0.05).

H. Optical sections of cleared tissue autofluorescence showing disorganization of cortical barrel fields in *Nf1$^{fl/fl}$;Emx1-Cre* and reduced Cux1+ neuron density in surrounding upper layer regions. Scale = 500μm.